
Analysis and evaluation of classification and segmentation of brain tumour images

M.P. Thiruvenkatasuresh*

Department of Computer Science and Engineering,
Excel Engineering College,
Namakkal, Tamilnadu, India
Email: mpthiruvenkatasuresh0773@gmail.com

*Corresponding author

V. Venkatachalam

Erode Sengunthar Engineering College,
Erode, Tamilnadu, India
Email: profdrv@gmail.com

Abstract: Apparently, the development of a model to detect the tumour part in brain images is of utmost significance. In the initial phase of our work, brain tumour database images have occurred in the preprocessing module using adaptive median filter technique to gain clarity of the image. In addition to the preprocessing process, feature extraction techniques are applied and extracted to the features then the classification method as support vector machine (SVM) classifier is used to classify the images as normal and abnormal. After classification, the abnormal images are observed for segmentation process using fuzzy c-means (FCM) clustering process along with the occupied optimisation methods. For optimising centroid, the FCM used social spider optimisation (SSO) technique with genetic algorithm. The proposed scheme has attained the maximum accuracy when compared to existing classification technique ANFIS and segmentation technique FCM (GWO).

Keywords: brain tumour images; support vector machine; SVM; fuzzy c-means; FCM; social spider optimisation; SSO; genetic algorithm; GA.

Reference to this paper should be made as follows: Thiruvenkatasuresh, M.P. and Venkatachalam, V. (2019) 'Analysis and evaluation of classification and segmentation of brain tumour images', *Int. J. Biomedical Engineering and Technology*, Vol. 30, No. 2, pp.153–178.

Biographical notes: M.P. Thiruvenkatasuresh received his BE in Computer Science and Engineering from the Madras University, Chennai, Tamilnadu, India in 1994 and ME in Computer Science and Engineering at the Annamalai University, Chidamparam, Tamilnadu, India in 2005. He is pursuing his PhD in Information and Communication – Computer Science and Engineering in Anna University, Chennai. He is currently working as an Associate Professor in the Department of Computer Science and Engineering, Excel Engineering College, Salem, Tamilnadu, India. He has 16 years of teaching experience and five years in research. His research interests are image and video processing, data mining and cloud computing.

V. Venkatachalam received his BE in Electronics and Communication Engineering from the Bharathiyar University, Coimbatore, Tamilnadu, India in 1989, MS in Software Systems in Birla Institute of Technology, Pilani, India in 1996 and MTech in Computer Science and Engineering at the Regional Engineering College, Trichy, Tamilnadu, India in 2004. He received his PhD in Computer Networks-Network Security under Information and Communication Engineering at the Anna University Chennai in 2009. He is currently working as a Principal at the Erode Sengunthar Engineering College, Erode, Tamilnadu, India. He has 26 years of teaching experience and 12 years in research. His research interests are network security, cryptography, database management, image and video processing and cloud computing.

1 Introduction

Medical image processing has been improved as a greatest challenging and developing field nowadays, the processing of MRI images is one of the important parts of this field (Al-Azzawi and Sabir, 2015). There are few distinct information mining calculations like order, affiliation run mining and bunching are created to concentrate what is called pieces of learning from expansive arrangements of data (Deepa et al., 2014). Though tumours can occur in any parts of the body, brain tumour can be considered as one of the serious and life-threatening tumours. In actual terms, it is created either by the abnormal and uncontrolled cell division within the brain or from cancers primarily present in other parts of the body (Charutha and Jayashree, 2014). Since the detection of brain tumours is generally a more complex task than the detection of any other image object, pattern recognition usually relies on the shape of required objects. Since the shape of tumour varies in each case, other properties have to be made use of (Dvorak et al., 2013). Many proposed automatic tumour detection techniques are based on fusion of complimentary information of different MRI modalities (Capelle et al., 2004). Classification methods such as neural network and support vector machine (SVM), and extraction of features, including shape-based and texture-based, were proposed for the purpose of automatic tumour segmentation (Iftekharruddin et al., 2009; Padma and Sukanesh, 2011). The AdaBoost classifier is used to find the best combination of features for classification of the image voxels into tumour and normal (Ghanavati et al., 2012). Brain tumour can be diagnosed by taking into account the personal and family medical history and also by physical examination, brain CT/MRI scan, brain angiogram, spinal tap biopsy, etc., (Aswathy et al., 2014). A non-automated segmentation process is often subject to variations, not only between different radiologists but also by the same expert (Porz et al., 2014; Hamamci et al., 2012). Surface element alludes to the spatial entomb connections for the fundamental components of a picture. Surface methods can be named as statistical, structural, model-based and signal processing techniques (Poonguzhali and Ravindran, 2007). There emerges a requirement for including a name or other data to every picture in the database, for the explanation of every picture. Henceforth, it is truly a tedious assignment to utilise distinctive watchwords for comment of every picture in a colossal database (Senthilkumar and Ezhilarasi, 2016). Self-arranging guide to MRI pictures of bosom malignancy. Utilising the prepared with kind hearted or dangerous flag qualities were effectively recognised and they could imagine injury cross-segments with pseudo-hues (Lim et al., 2010). Moreover, the neoplastic tumour tends to vary

significantly in geometric properties, location and degree of enhancement among patients, making the segmentation and characterisation of brain abnormalities a very demanding, complex and a very time consuming task (Kanas et al., 2015). The availability of the brain web atlas was a major advance in the practical application of the model briefly described in detail below. This allowed the application of the model to anatomically correct brains (Murray, 2012). Biomedical designing is the examination and innovation improvement identified with the medicinal field. It requires information of essential sciences, fundamental gadgets, instrumentation, programming outline and improvement, mechanics, biomaterials, human life systems and physiology (Chawla and Duhan, 2014). A most important aspect in clinical practice is the early detection and classification of brain tumours. Though several researchers have proposed assorted techniques for the classification of brain tumours based on varied sources of information (Murugesan and Sukanesh, 2009; Majo et al., 2004). Image segmentation plays a major role in biomedical imaging applications such as the enumeration of tissue volumes diagnosis, confinement of pathology analysis of anatomical structure, treatment planning, partial volume improvement of practical imaging data and computer incorporated surgery (Kavitha and Chellamuthu, 2013). Many of the image processing techniques are based on threshold based, edge based, region based methods and cluster based. Due to the distribution of intensity in tissue being complex, threshold determination becomes a difficult task (Preetha and Suresh, 2014; Lemieux et al., 1999). The motivation of the research work is primary brain tumours constitute a heterogeneous set of tumours associated with variable behaviours, symptoms, origins and malignancy. The existing works use the brain images for pre processing and some features are extracted from the preprocessed images to carry out the classification procedure. The existing classification techniques such as, adaptive neuro fuzzy inference system (ANFIS) and the feed forward back propagation (FFBN) neural network process the extracted features that are given as the input to them and help in classifying the tumour as well as the non-tumour parts of brain images. But, this process consumes the maximum computation time. After the classification process gets finished, the segmentation process is performed using region growing (RG) method. In this method, the seed points and the threshold value are chosen randomly. However, the segmentation process suffers from some drawbacks like, the pixel values are compared with the value of neighbours every time and the obtained accuracy is also found to be small. To overcome the problems, we will introduce new techniques for brain tumour detection process. The main purpose of the study is to identify tumour in brain images and improve the performance measures with medical applications. Overview of this paper: Section 2 elaborates explanations concerning the literary reviews is given. Section 3 is rich with colourful data on the epoch-making technique. In Section 4, the outcomes and its consequent debate is exhibited. This section contains the cheering outcomes and the execution procedure along with the evaluation section. This compares the existing technique with the current approach and establishes without doubt that our dream scheme is clear and unbeatable over the other current techniques. The section ends with a perfect conclusion.

1.1 Objectives of proposed work

- To study the brain tumour image detection process four different phases are considered.

- To extract the meaning full information in all the database images.
- Tumour classification process mainly used SVM technique and segmentation approach uses optimal FCM.
- From the analysis achieves maximum accuracy and the performance metrics in our proposed work compared to existing paper.

2 Literature review

The literary domain is flooded with various fantastic techniques spearheaded with the intention of promoting the brain tumour detection process. Recounted below are some of modern noteworthy works related to the captioned topic.

In 2016, Chandra and Ramchand have proposed the detection of brain tumour as a very common fatality in current scenario of healthcare society since brain tumour is an abnormal mass of tissue in which cells grow and multiply uncontrollably, image segmentation was used to extract the abnormal tumour portion in brain. They were apparently unregulated by mechanisms in control cells. Though several techniques have been developed for detection of tumour in brain, the main concentration of the techniques which use image segmentation helps to detect brain tumour. Tumour classification and segmentation from brain computed tomography image data is an important but time consuming task performed by medical experts.

In 2015, Renjith et al. have proposed an improved method based on magnetic resonance imaging (MRI) brain image classification and image segmentation approach. Automated classification was encouraged due to the need of high accuracy when dealing with a human life. Firstly, image pre-processing is used to enhance the image quality. Secondly, dual-tree complex wavelet transform multi-scale decomposition is used for the texture analysis of an image. Feature extraction extracts features from an image using grey-level co-occurrence matrix (GLCM). To proceed further, the neuro-fuzzy technique is used to classify the stages of brain tumour as benign, malignant or normal based on texture features. Finally, tumour location is detected using Otsu thresholding and the classifier performance evaluation is done based on classification accuracies. The simulated results showed that the proposed classifier provides better accuracy than previous method.

In 2015, Suganami et al. have suggested the physicochemical properties of liposomal formulated phospholipids conjugated ICG. This was denoted by LP-iDOPE, as a clinically translatable NIR imaging nanoparticle for brain tumours. The properties of LP-iDOPE may enable neurosurgeons to achieve more accurate identification and more complete resection of brain tumour.

In 2015, Shanthakumar Ganeshkumar have suggested the ANFIS based on the automatic seed point selection range. The pixels intensity of the proposed algorithm did not depend on the type of tumour. The tumour's segmentation results are evaluated based on various criteria, including similarity index (SI), overlap fraction (OF), extra fraction (EF) and positive predictive value (PPV), which corresponded to values of 0.817%, 0.817%, 0.182%, and 0.817%, respectively. These results indicate that the proposed approach performs better compared to many conventional processes. The significance of the work was the differentiation of brain abnormalities from the healthy brain tissue.

In 2015, Aslama et al. have proposed the improved edge detection algorithm for brain-tumour segmentation. The presentation was based on Sobel edge detection which combines the Sobel method with image dependent thresholding method, and finds different regions using closed contour algorithm. Finally, tumours extraction from the image was done using intensity information within the closed contours. The algorithm was implemented in C and its performance was measured objectively as well as subjectively. Simulation results showed that the proposed algorithm gave superior performance over conventional segmentation methods. For comparative analysis, various parameters are used to demonstrate the superiority of proposed method over the conventional ones.

In 2015, Yacin and Vennila have proposed the two calculations were utilised, extended state Kalman filter which utilises adjusted nonlinear powerful model and monastery created manufactured ECG signs and fast ICA which utilises the request of kurtosis. At long last, Hilbert-Huang transform (HHT) was connected to remove flag and it depicts the nonlinear and non-stationary nature of signs by quick recurrence which uncovers the intra-wave recurrence regulations. Likewise the efficiencies of these strategies were looked at in view of couple of vital models; for example, yield waveforms, PSNR and vitality capacity of the extricated flag. In light of these discoveries the best strategy in separating foetal ECG from clamour polluted source signs was exhibited.

In 2015, Rajalakshmi and Prabha have proposed the shading changed over division by new cross breed developmental grouping calculation which is the blend of weighted firefly and K-implies calculation to beat neighbourhood optima issues in firefly calculation. Promote irregular bunch initialisation is additionally demonstrated. The consequences of the reproduction demonstrate that the execution of the proposed calculation has preferable division precision over alternate calculations, for example, shading changed over PSO-K-means and K-implies grouping calculation. The execution of the technique is assessed utilising order exactness, affectability, specificity and receiver operating characteristic (ROC) bends. The outcomes demonstrated that the most noteworthy grouping exactness of more prominent than 98% is gotten for the proposed indicative model, and this is exceptionally encouraging contrasted with the already reported outcomes.

In 2014, Singla et al. have suggested the four distinctive glimmering frequencies in low-recurrence district were utilised to inspire the SSVEPs and were shown on a liquid crystal display (LCD) screen utilising LabVIEW. Four jolts hues, green, red, blue and violet, were utilised as a part of this review to research the impact of shading on SSVEPs. The EEG signals recorded from the occipital locale were portioned into 1 second windows and components were removed by utilising wavelet change. Bolster vector machines (SVMs) are utilised for characterisation. In shading examination, SSVEP with the violet shading demonstrated higher exactness than that with other boosts.

In 2014, Zeljko et al. had explained the MRI or CT scan images are primary follow up diagnostic tools. Here a neurologic exam indicates a possibility of a primary or metastatic brain tumour existence. The tumour tissue is spotted mainly in brighter colours than rest of the regions in brain. An automated algorithm for brain tumour detection and medical doctors' assistance is facilitated and accelerated based on this observation. The diagnosis procedure has been developed and tested initially on images obtained from the patients with diagnosed tumours and healthy subjects.

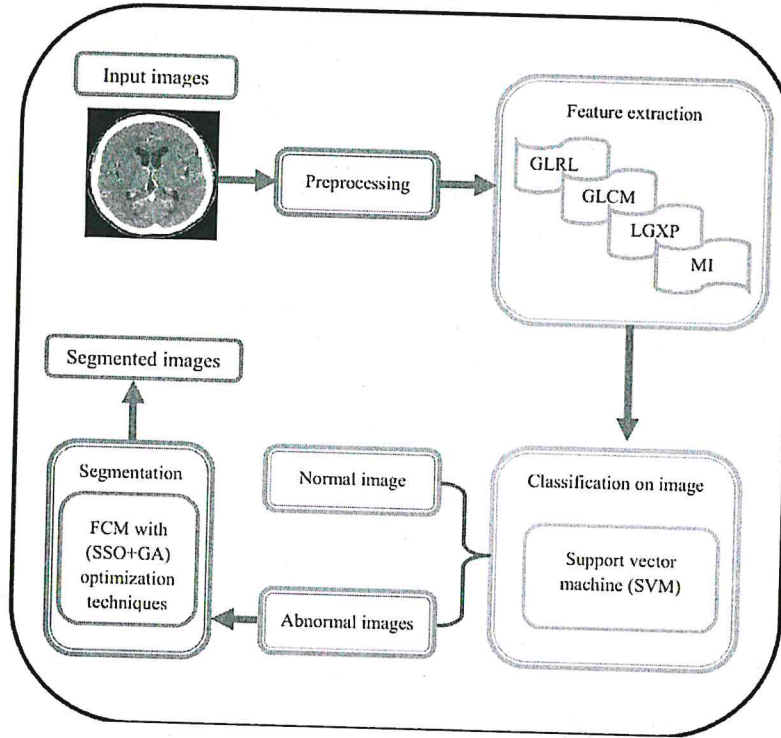
In 2014, Halder et al. have suggested the efficient brain tumour detection method. This can act as an aid to detect tumour and locate it in the brain MRI images. The method extracts the tumour by using K-means algorithm followed by object labelling algorithm with some preprocessing steps (median filtering and morphological operation) used for tumour detection purpose. It can be observed from the experimental results that the proposed method gives better result in comparison to other techniques.

Application of adaptive neuro-fuzzy inference systems for MR image classification and tumour detection by Rajasekaran and Sri Meena (2012) proposed that ANFIS is connected for grouping and location. Basic leadership was performed in two phases: highlight extraction utilising principal component analysis (PCA) and ANFIS prepared with the back propagation inclination plunge technique in mix with slightest squares strategy. The execution of the ANFIS classifier is assessed as far as preparing execution and grouping exactnesses and the outcomes affirms that proposed ANFIS has potential in identifying the tumours.

In 2012, Gandhi et al. have proposed the trial display and an arrangement of stipulations for comprehension neural movement in human mind while recognising well known countenances, and relationship amongst acknowledgment and different parts of face preparing. Dynamical symbolism boosts of well known and new faces were appeared to solid people and were requested that remember them as fast and precisely as could be expected under the circumstances. Comes about got from the non-parametric examination of the recorded multivariate information showed that procedure of auxiliary translating of new faces happening inside the mind is postponed in correlation with recognisable face most likely because of couple of unmistakable data that they get from seen confronts seem to impact the preparing execution of cerebrum amid the errand.

3 Proposed method

The objective of this research work is to help the development of model to detect the tumour part in brain images. The brain tumour database is initially considered to the pre processing steps which are applied over the images. The adaptive median filter technique is used for increasing the clarity of the image. After preprocessing steps, the extraction of meaning full information such as GLCM, local Gabor XOR pattern (LGXP), grey-level run-length matrix (GLRLM) and maximum intensity (MI) from medical images is carried out. After the completion of feature extraction the extracted features are classified using SVM classifier. After the classification process, the brain tumour image has been taken in the segmentation method. This is done by using fuzzy c-means (FCM) clustering process which employing the optimisation method. For the purpose of optimising the centroid of FCM by using social spider optimisation (SSO) technique with genetic algorithm (GA), these optimisation techniques are used to improve the segmentation accuracy. Finally, by utilising the optimal centroid the extracted tumour part of the image is obtained. When compared to existing classification technique ANFIS and segmentation technique FCM the proposed scheme attains the maximum accuracy. The block diagram of the proposed method is given here under in Figure 1.

Figure 1 Block diagram of proposed methodology (see online version for colours)

3.1 Preprocessing

Adaptive median filter is used to empower the flexibility of the filter. This helps to change its size as it needs to be seen on the guess of local noise density. The adaptive median filter is dependent on a trans-conductance comparator, where immersion current can be altered to go about as a local weight operator. There is a kind of median filter known as adaptive median filter since the size of the filter is adjusted to the local noise content. If image is noisy and target pixels neighbouring pixel worth is somewhere around 0's and 255's in this filter, then we supplant pixel esteem with the median value.

Let $L_{i,j}$ which locates at (i, j) , be the grey intensity of an $A \times D$ image L and $\min \max K \times K$ be the dynamic range of L , i.e., $\min i, j \max K \leq x \leq K$ for all (i, j) which accords to the following rule:

$$(i, j) \in C = \{1, \dots, A\} \times \{1, \dots, D\} \quad (1)$$

In the conventional noise model, we assume Y is the noisy image, the model is given by:

$$Y_{i,j} = \begin{cases} K_{\min} & \text{with percentage } p \\ K_{\max} & \text{with percentage } q \\ L_{i,j} & \text{with percentage } 1-p-q \end{cases} \quad (2)$$

where $rate = p + q$ means the noise level in image and assume the filtering window O_{ij} is a window of size $(2C + 1) \times (2C + 1)$ centred at position at (i, j) , O_{ij} can be written as:

$$O_{i,j} = \{L_{i-C,i-C}, \dots, x_{i,j}, \dots, x_{i+C,j+C}\} \quad (3)$$

Let $w = 2C + 1 \leq O \max$. The filter tries to improve the output image Y_{ij} the median in the window.

3.2 Feature extraction

The feature extraction technique includes the investigation of brain CT images. The spectral analysis method is conveyed for this image feature extraction. It implies by feature extraction the adaptation of the input data into the set of features. The features that are seriously dealt with in our examination are:

- GLRLM
- GLCM
- LGXP
- MI.

3.2.1 Grey-level run-length matrix

A matrix from which the texture features can be extricated for texture examination is known as GLRLM. A texture comprehension is an example of grey intensity pixel in a specific heading from the reference pixels. The quantity of the nearby pixels that have the same grey force in a specific direction is termed as run length. GLRLM is a two dimensional matrix where every element $z(u, v / \theta)$ is the number of elements v with the intensity u in the direction θ . The GLRLM is developed as takes after:

$$K(\theta) = (r(u, v) / \theta), 0 \leq u \leq N_r, 0 \leq v \leq K \max \quad (4)$$

where N_r the maximum is grey level, $K \max$ is the maximum length and u, v is a matrix size values.

GLRLM obtains more than a few statistics by employing the grey co-props function. These statistics provides information about the texture of an image. The statistics are stated below:

a Short run emphasis (SRE)

$$SRE = \frac{1}{n_g} \sum_{u=1}^R \sum_{v=1}^S \frac{z(u, v)}{v^2} \quad (5)$$

The SRE is highly dependent on the occurrence of short runs and is expected large for fine textures.

b Long run emphasis (LRE)

$$LRE = \frac{1}{n_g} \sum_{u=1}^R \sum_{v=1}^S z(u, v) * v^2 \quad (6)$$

c Grey-level non-uniformity (GLN)

GLN measures the similarity of grey level values throughout the image. The GLN is expected small if the grey level values are alike throughout the image.

$$GLN = \frac{1}{n_g} \sum_{u=1}^R \left(\sum_{v=1}^S z(u, v) \right)^2 \quad (7)$$

d Run length non-uniformity (RLN)

Measures the length's similitude of keeps running all through the image, The RLN is expected little if the run lengths are indistinguishable all through the image.

$$RLN = \frac{1}{n_g} \sum_{u=1}^S \sum_{v=1}^R (z(u, v))^2 \quad (8)$$

e Run percentage (RP)

$$RP = \frac{n_g}{z(u, v) \times v} \quad (9)$$

The homogeneity and the circulation of keep running of an image in a specific direction the RP is the biggest when the length of runs is 1 for every grey levels in specific direction.

3.2.2 Grey level co-occurrence matrix

A GLCM invariably represents a matrix where the number of rows and columns are equivalent to the number of grey levels, G , in the image. The matrix element $p(i, j | d_1, d_2)$ symbolises the equivalent segregated by a pixel distance (d_1 and d_2). The GLCMs are capable of gathering sufficient statistics from them. This is achieved by means of the grey co-props function, which furnishes the details regarding the texture of an image. It can be categorised as follows:

a Energy

The angular second moment, alternatively known as the uniformity or energy, signifies the total of squares of the entries in GLCM. It is known by the name 'uniformity' where the range of energy is defined as $[0.1]$. The value of energy for a fixed image is considered to be one. The equation for evaluating the energy is furnished as follows:

$$Energy = \sum_{i,j} p(i, j)^2 \quad (10)$$

where $p(i, j)$ is the pixel value at the point i, j of the texture image of size $(M \times N)$.

b Entropy

The entropy lends a helping hand to represent the texture image. This helps to determine the distribution change in a region of the image. The corresponding parameter helps for an efficient estimation of the disorder of an image. When the

image appearance is not textually similar, a number of GLCM elements contain negligible value, thereby revealing the fact that the entropy is unduly large. The entropy is estimated as per the following equation:

$$Ent = \sum_{i,j} p(i, j) \log(p(i, j)) \quad (11)$$

c Cluster shade

$$CS = \sum_{i,j} ((i - \alpha_i) + (j - \alpha_j))^3 T(i, j) \quad (12)$$

d Homogeneity

The homogeneity evaluation is the uniformity of non-zero entries in GLCM. When the variations in grey values are higher, the GLCM homogeneity is lower. This facilitates a superior GLCM contrast. The homogeneity is within the range of [0, 1]. If there is only a moderate variation of the image, then the homogeneity is greater and if the image is not at all changed, then the homogeneity is equivalent to one.

$$Homogeneity = \sum_{i,j} \frac{P(i, j)}{[1 + (i - j)^2]} \quad (13)$$

e Maximum probability

$$Max\ probability = \max(p(i, j)) \quad (14)$$

3.2.3 Local Gabor XOR pattern

The phase part of Gabor is followed by LBP which gives LGXP. In LGXP, descriptor phases are quantised into the diverse ranges. The number of phase ranges is generated in order to devise the patterns dynamic to the deviations of Gabor phase, and hence extreme elevation is not possible. Every single phase value is quantised using the quantisation procedure. Subsequently, the LGXP operator is effectively utilised to the quantised phases of the central pixel and each of its neighbours. $LGXP_{v,w}^i = (q = 1, 2, \dots, q)$ denotes the pattern determined between $\phi_{v,w}(k)$ and its neighbour O_i is evaluated as illustrated below:

$$LGXP_{v,w}^i = p(\phi_{v,w}(O_c) XOR p(\phi_{v,w}(O_i))) \quad (15)$$

Here, $\phi_{v,w}(O_c)$ denotes the phase and $p(\phi_{v,w}(O_i))$ represents the quantised value of the phase and where $\phi_{v,w}(k)$ depicts the central pixel position in Gabor phase map with scale ω and orientation w , p represents the dimension of neighbourhood. At last, the consequential binary labels are concatenated jointly as local pattern of the central pixel.

$$LGXP_{v,w}(O_c) = [LGXP_{v,w}^q, LGXP_{v,w}^{q-1}, \dots, LGXP_{v,w}^1]_{binary} = \sum_{i=1}^q 2^{i-1} \cdot LGXP_{v,w}^i \quad (16)$$

At the end of LGXP procedure, an identical value is achieved and there is a repetition of relative task for every single block. Subsequently, for the feature extraction procedure, the features are furnished to fusion process.

3.2.4 Maximum intensity

The histogram of an image is mostly identified with a pixel's histogram force values in connection with the image processing connection. Moreover, it speaks to a graph portraying the number of pixels in an image at every last special force worth found in the relative image. Since there are 256 different achievable intensities for an 8-bit greyscale image, the histogram graphically offers 256 numbers portraying the designation of pixels among those greyscale values.

$$I = \max_{i=0}^{255} (\text{count of pixel intensity}) \quad (17)$$

3.3 Classification using SVM

The furnishing of GLCM, GLRLM, LGXP and minimum intensity features helps to achieve SVM for the purpose of classification. Here, by employing the feature is extorted from the earlier process and finds the effective use for the segregation of two classes. In order to perform the nonlinear process, the kernel functions are initiated in the SVM classification. The two vital stages in the SVM process are training stage and the testing phase.

3.3.1 Linear kernel function

Intuitively, better-quality segregation is achieved by hyper plane which has the maximum distance to the neighbouring training data point of any class. Linear kernel function in SVM procedure is efficiently employed which helps to construct the hyper plane equation. The statistical evaluation revealing huge margin overshoots the bane of dimensionality. When the training data is linearly detachable, it is possible to choose two hyper planes in such a manner that the data is segregated without points in between them, and thereafter an endeavour is made to reduce their distance. The two classes are linearly separable, thereby implying that it is feasible to locate at least one hyper plane defined by a vector with a bias, which is competent to separate the classes with zero error. The linear kernel function is represented as follows.

$$K(y, y_i) = y \cdot y_i \quad (18)$$

3.3.1.1 Steps involved in the SVM process

- 1 Hyper plane acting as the decision surface is defined as:

$$\sum_{i=1}^N \chi_i \cdot f_i \cdot K(y, y_i) = 0 \quad (19)$$

where y denotes a vector drawn from the input space, assumed to be a dimension as p_0 , χ_i is the Lagrange coefficient, f_i corresponding target output and $K(y, y_i)$ represents the inner product of two vectors induced in the feature space by input

vector y and input pattern y_i pertaining to the i^{th} example. This term is referred to as inner-product kernel.

$$w = \sum_{i=1}^N \chi_i \cdot f_i \cdot y_i, b = w \cdot y_k - f_k \quad (20)$$

- 2 Once the Lagrange multipliers are determined, the normal vector w and the threshold b can be derived from the Lagrange multipliers, where b is a bias? Because w can be computed via equation (11) from the training data before use, the amount of computation required to evaluate a linear SVM is constant in the number of non-zero support vectors.
- 3 The requirement of the kernel $K(y, y_i)$ function is selected as a linear kernel function. The function refers to the equation (10).
- 4 The Lagrange multipliers $\{\chi_i\}$ are still computed via a quadratic program. The nonlinearities alter the quadratic form, but the dual objective function as $U(\chi)$ is still quadratic in χ .

$$\min U(\chi) = \min \frac{1}{2} \sum_{i=1}^N \sum_{j=1}^N f_i f_j K(y_i, y_j) \chi_i \chi_j - \sum_{i=1}^N \chi_i \quad (21)$$

$$0 \leq \chi_i \leq C$$

$$\sum_{i=1}^N \chi_i \cdot f_i = 0$$

Finally, the normal and abnormal images are classified using this SVM classification technique. After classification segmentation process is considered in below sections.

3.4 Segmentation process

With the aid of mighty FCM clustering technique we have viably isolated the tumour image with optimisation procedure in this area. This delicate (fuzzy) division strategy holds considerably more data than hard division strategies and provides flexibility through fuzzy classification of pixels where pixels are permitted to have a place with various clusters with a membership degree somewhere around 0 and 1. The algorithm, which is an iterative advancement, minimises the objective function where the FCM is generally utilised for clustering. Here the execution of FCM relies on the determination of initial cluster centre or membership value to the tumour image pixel values. The FCM algorithm begins with an arrangement of initial cluster centres (or) arbitrary membership values. To optimise the cluster centre utilising SSO, GA techniques are used. The tumour's characterisation image is assigned as the input to the division process to coerce the tumour piece of the image, which is exhibited in Figure 4.

3.4.1 FCM clustering process

FCM algorithm allows data to have a place with two or more clusters with different membership coefficient. FCM clustering is an iterative procedure, where at the start, fuzzy partition matrix is created and initial fuzzy cluster centres are computed. As the iteration progresses, the cluster centres and the membership grade point are overhauled and the objective function is minimised. This helps to locate the best area for the clusters. Here, we have mentioned the FCM algorithm steps. FCM has been utilised by accomplishing a part of the delicate division of MR images and for the estimation of partial volumes. It is formulated as the accompanying minimisation objective function concerning the membership function x and the centroids y .

The parameter m controls the fuzziness of subsequent segment, and $m = 2$ is utilised as a part of this study. The objective function is minimised when pixels are near to the focuses of their clusters and are relegated high membership values, and low membership values are allotted to pixels with far from the focuses of their clusters. The membership function speaks to the probability that a pixel fits in with a specific cluster.

3.4.1.1 Steps for FCM algorithm

- 1 Let $u = \{u_1, u_2, \dots, u_n\}$ be the set of data points and $c = \{c_1, c_2, \dots, c_n\}$ be the set of centres.
- 2 For select the cluster centre or centroid in the segmentation process using SSO technique.
- 3 Compute the objective function of the fuzzy process using below function

$$J_m = \sum_{i=1}^n \sum_{j=1}^c R_{ij}^m \|u_i - c_j\|^2 \quad (22)$$

- 4 Calculate the fuzzy membership function R_{ij} using

$$R_{ij} = \frac{1}{\sum_k (d_{ij}/d_{ik})^{(2(m-1))}} \quad (23)$$

- 5 Compute the fuzzy centres c_j

$$c_j = \left(\frac{\sum_{i=1}^n (R_{ij})^m u_i}{\sum_{i=1}^n (R_{ij})^m} \right) \quad \forall j = 1, 2, \dots, c \quad (24)$$

- 6 Repeat Step 4 and 5 until the maximum of J_m value is achieved or $\|R^{(k+1)} - R^k\| < \beta$.

3.4.2 Centroid optimisation using SSO with GA

By applying the optimisation technique, the execution of this process attains the segmented image. In the centroid optimisation, the maximum sensitivity is obtained in SSO with GA.

Table 1 Pseudo code for SSO algorithm

<i>Step 1:</i> Initialisation
<i>Step 2:</i> Fitness computation (F_i)
<i>Step 3:</i> Based on fitness update the new spider population
{
Find the number of female and male spiders (R_f and R_m)
Evaluate the weight (w_i) based on the fitness (F_i)
Fitness based initialises the population ($f_{i,j}^0$ and $m_{k,j}^0$)
Find the cooperative operator
<i>Female cooperative operator</i> (f_i^{k+1})
<i>Male cooperative operator</i> (m_i^{k+1})
Mating process find the probability (po_{Ri})
Find the fitness for the new spider solution ($F_{i(new)}$)
}
<i>Step 5:</i> Store the best spider of the solution so far attained
Stop until optimal solution ($F_{optimal}$) attained
Iteration = Iteration + 1
<i>Step 7:</i> Find the error value (E_i)

It is invariably presumed by SSO that the entire search space represents a communal web, where all the social-spiders associate with one another. In the novel technique, every single solution in the search space characterises a spider location in the communal web. Every spider is given a weight in accordance with the fitness value of the solution which is signified by social-spider approach for the SSO process illustrated by the captioned pseudo code.

3.4.2.1 Initialisation process

In the district developing procedure, we pick the seed point and the centroid fragment of the image. Here, we introduce the centroid c_i and certain algorithm parameters, for example, a , A , and C as coefficient vectors.

3.4.2.2 Fitness evaluation

In every square of the image, we continue to find the fitness F_i in a portioned part and here the fitness is the most extreme precision of fragmented part. The precision is discovered utilising the parameters, for example, true positive (TP), true negative (TN), false positive (FP) and false negative (FN).

3.4.2.3 New population updation by using following procedure

The novel technique envisages two diverse search agents (spiders) namely the males and females. Every single individual performs a set of diverse evolutionary operators which imitate the various cooperative trends which are habitually presumed inside the colony. This varies with the gender. Taking R as the total number of n -dimensional colony members, the number of male R_m and females R_f spiders in the total population R is defined.

$$R_f = \text{floor}[0.9 - \text{rand}.025).R] \text{ and } R_m = R - R_f \quad (25)$$

where rand is a random number between $[0, 1]$ and $\text{floor}(\cdot)$ maps a real number to an integer number.

3.4.2.4 Weight assignment

With the biological metaphor, the spider size represents the unique feature which estimates the individual skills which helps to carry out its delegated functions efficiently. Each and every individual (spider) is allocated a weight w_i which characterises the solution quality which is related to the spider i (regardless of the gender) of the population V . The weight of each and every spider of V is evaluated by means of equation (4).

$$w_i = \frac{F(V_i) - \text{worst}_V}{\text{best}_V - \text{worst}_V} \quad (26)$$

where $F(V_i)$ is the fitness value obtained by evaluation of the spider position V_i with regard to the objective function F . The values worst_V and best_V are calculated as below equation.

$$\text{best}_V = \min_{k=\{1,2,\dots,N\}} (F(V_k)) \text{ and } \text{worst}_V = \max_{k=\{1,2,\dots,N\}} (F(V_k)) \quad (27)$$

3.4.2.5 Fitness-based initialises the population

The algorithm begins by initialising the set S of R spider positions each spider position f_i and m_i is a dimensional vector containing the parameter values to be optimised. Such values are randomly and uniformly distributed between the pre specified lower initial parameter bound po_j^{low} and the upper initial parameter bound po_j^{high} just as it distributed by using equations (5) and (6).

$$f_{i,j}^0 = po_j^{\text{low}} + \text{rand}(0, 1) \cdot (po_j^{\text{high}} - po_j^{\text{low}}) \quad (i = 1, 2, \dots, R_m, j = 1, 2, \dots, n) \quad (28)$$

$$m_{k,j}^0 = po_j^{\text{low}} + \text{rand}(0, 1) \cdot (po_j^{\text{high}} - po_j^{\text{low}}) \quad (k = 1, 2, \dots, R_m, j = 1, 2, \dots, n) \quad (29)$$

where i, j and k are the parameter and individual indexes respectively. Whereas zero signals have initial population hence $f_{i,j}$ is the j^{th} parameter of the i^{th} female spider position.

3.4.2.6 Cooperative operators

3.4.2.6.1 Female cooperative operator

The female spiders exhibit a charm or disgust over others as an irrespective of the sexual orientation. With a specific female spider, the corresponding charm or disgust is habitually generated over the other spiders. This is evident by their vibrations which are released over the communal web. As these vibrations invariably rely on weight and distance of the members which have instigated them, sturdy tremors are generated by the giant spiders or the neighbouring members which are situated next to the person which observes them. The former case is concerned with the transformation with respect to the closest member to i which possesses a greater weight and generates the vibration $Vibrc_i$. The latter case involves the modification with regard to the best individual of the whole population V which generates and produces the vibration $Vibrb_i$. The female vibration $Vibrc_i$ and $Vibrb_i$ are estimated by means of equation (8).

$$Vibrc_i = w_c \cdot e^{-d_{i,c}^2} \quad Vibrb_i = w_b \cdot e^{-d_{i,b}^2} \quad (30)$$

The vibration $Vibrc_i$ is perceived by the individual $i(V_i)$ as a result of the information transmitted by the member $c(V_c)$ who is an individual that has two important characteristics: it is the nearest member to i and possesses a higher weight in comparison to $i(w_c > w_i)$. The vibration $Vibrb_i$ are perceived by the individual i as a result of the information transmitted by the member $b(V_b)$ with b being the individual holding the best weight that ids fitness of the entire population V such that $w_b = \max_{k \in \{1,2,\dots,N\}} w(k)$.

If rm is smaller than threshold PF an attraction movement is generated; otherwise a repulsion movement is produced. Therefore, such operator can be modelled as follows:

$$f_i^{k+1} = \begin{cases} f_i^k + \alpha \cdot Vibrc_i \cdot (V_c - f_i^k) + \beta \cdot Vibrb_i \cdot (V_b - f_i^k) + \delta \cdot (rand - 1/2) \\ \text{with probability PF} \\ f_i^k - \alpha \cdot Vibrc_i \cdot (V_c - f_i^k) + \beta \cdot Vibrb_i \cdot (V_b - f_i^k) + \delta \cdot (rand - 1/2) \\ \text{with probability } 1 - PF \end{cases} \quad (31)$$

where α , β , δ and $rand$ are random numbers between $[0, 1]$ whereas k represents the iteration number. The individual v_c and v_b represent the nearest member to i that holds a higher weight and the best individual of entire population V .

3.4.2.6.2 Male cooperative operator

Male members possess a weight value greater the median value within the male population. This is deemed as the dominant individuals D . Conversely, those within the median value are considered as the non-dominant ND males. With the intention of performing the corresponding evaluation, the male population $M(M = \{m_1, m_2, \dots, m_{N_m}\})$ is orchestrated in accordance with their weight value in the descending order. Hence, the individual having weight $w_{R_{f+m}}$ situated in the middle is taken as the median male member and the vibration of the male $Vibrf_i$ evaluated with the help of equation (10) given below. The vibration $Vibrf_i$ observed by the individual $i(V_i)$ on account of the data communicated by the member $f(V_f)$ with f being the closest female individual to i .

$$Vibrf_i = w_f \cdot e^{-d_{i,f}^2} \quad (32)$$

Since indexes of the male population M in regard to the entire population V are increased by the number of female members R_f , the median weight is indexed by R_{f+m} . According to this, change of positions for the male spider can be modelled as follows:

$$m_i^{k+1} = \begin{cases} m_i^k + \alpha \cdot Vibrf_i \cdot (R_f - m_i^k) + \delta \cdot (rand - 1/2) & \text{if } w_{R_{f+i}} > w_{R_{f+m}} \\ m_i^k + \alpha \cdot \left(\frac{\sum_{h=1}^{R_m} m_h^k \cdot w_{R_{f+h}}}{\sum_{h=1}^{R_m} w_{R_{f+h}}} - m_i^k \right) & \text{if } w_{R_{f+i}} \leq w_{R_{f+m}} \end{cases} \quad (33)$$

where the individual R_f represents the nearest female individual to the male member i whereas.

$$\left(\frac{\sum_{h=1}^{R_m} m_h^k \cdot w_{R_{f+h}}}{\sum_{h=1}^{R_m} w_{R_{f+h}}} \right) \text{ corresponds in the weighted mean of male population}$$

M .

By employing the above-mentioned operator, it generates two diverse phenomena. In the former, the set D of particles is fascinating to others with the intention of inciting the act of mating, which in effect permits the integration of diversity into the population. In latter, the set ND of particles is fascinating to the weighted mean of male population M , and this phenomenon is effectively employed to moderately regulate the search procedure. This is in accordance with the average performance of a subgroup of the population.

3.4.2.7 Mating process

The mating in a social-spider colony is carried out by the leading males and the female members. In such a scenario, when a leading male m_g spider ($g \in D$) finds a set E^g of female members within a specified range r (which is considered as the range of mating), it mates, producing a new brood V_{new} which is produced due to an account of the entire elements of the set T^g which, in turn, has been created by the union $E^g \cup m_g$. It is pertinent to note that if the set E^g is vacant, the mating function has to be abandoned. The range r is concisely described as the radius which is dependent on the dimension of search space. Now the female ($F = \{f_1, f_2, \dots, f_{R_f}\}$) and male ($M = \{m_1, m_2, \dots, m_{R_m}\}$) are randomly initialised where $V = \{V_1 = f_1, V_2 = f_2, \dots, V_{R_f} = f_{R_f}, V_{R_{f+1}} = m_1, V_{R_{f+2}} = m_2, \dots, V_R = m_{R_m}\}$ and the radius mating is calculated.

$$r = \frac{\sum_{j=1}^n (po_j^{high} - po_j^{low})}{2 \cdot n} \quad (34)$$

In the mating process, the weight of each involved spider (elements of T^g) defines the probability to influence each individual into the new brood. The spiders with a heavy weight holding capacity is more likely to influence the new product, while elements with

lighter weight have a lower probability. The influence probability PO_{Vi} of each member is assigned by the roulette method, which is defined as follows:

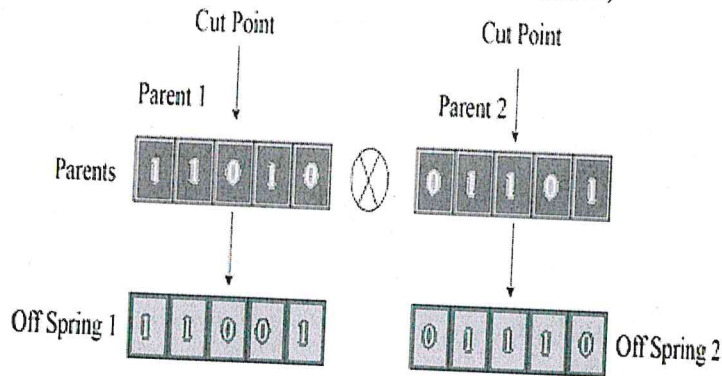
$$PO_{Vi} = \frac{w_i}{\sum_{j \in T^k} w_j} \quad \text{where } i \in T^g \quad (35)$$

With the generation of the new spider, it is contrasted with new spider candidate V_{new} have the worst spider V_{wo} of the colony, depending on their weight values. If the new spider is superior to the worst spider, the worst spider is substituted by new one. Unless the new spider is eliminated, the population remains unmodified. On the contrary, in the case of substitution, the new spider takes control of the gender and index from the substituted spider. This ensures that the whole population V preserves the original rate between female and male members. In accordance with this procedure, the optimum hidden layer and neuron of the neural network procedure evaluation is done.

3.4.2.8 Crossover updation process

By utilising the better set of solutions (chromosomes) an offspring is produced by crossover operation. Every two individuals are chosen from the better set of chromosome to produce two new offspring by single crossover point. Figure 2 shows the crossover operation.

Figure 2 Crossover single point operation (see online version for colours)



3.4.2.9 Mutation process

The mutation operator preserves diversification in the search and it chooses the random mutation. Mutation is a genetic operator used to maintain genetic diversity from one generation of a population of GA chromosomes to the next which is analogous to biological mutation. Mutation alters one or more gene values in a chromosome from its initial state and the solution tends to change entirely from the previous solution. Hence, GA reaches better solution by using mutation. Mutation occurs during evolution according to a user-definable mutation probability that is to be set low.

If set is too high, the search turns into a primitive random search. This operator is applied to each offspring in the population with a predetermined probability. The obtained new set of individuals is then fed to the mutation operator. Further, two individuals are newly obtained from the single point mutation operator. The updating process is continued till the satisfied presentation.

3.4.3 Optimal centroid to the FCM

The last process is the segmentation process, the value attained from the optimal centroid, the computation process leads to a precise extorted tumour part of the image.

4 Results and discussion

The proposed brain tumour classification and segmentation are experimented in the working platform of MATLAB 2014 with the system configurations as i5 processor with 4 GB RAM. The evaluation is done in respect of classification as well as the segmentation. Subsequently in the segmentation, the performance evaluation is carried out in terms of sensitivity, specificity, accuracy, random index (RI), global consistency error (GCE) and the variation of information (VI). By utilising the SVM technique, it helps to classify the tumour part of image and FCM with SSO + GA techniques being employed to predict the centroid. This produces better results, when the proposed work is compared to the existing work in terms of FCM with GWO algorithm.

4.1 CT image dataset description

By employing the CT image dataset, the innovative tumour detection approach helps to compile the public accessible sources and it encompasses the brain CT images including the tumour and non-tumour images. The CT image dataset have utilised in our proposed tumour detection technique is collected from M/s Aarthi scans (3D multi slice CT scanner), Tirunelveli, India. This image dataset contains brain CT images which involve both tumour images (205 numbers) and non-tumour images (78 numbers). The dataset of brain images, in essence, is divided into two distinct segments like the training and testing datasets. The training dataset, in turn, is effectively employed to fragment the brain tumour images. Here the testing dataset elegantly executes the function of assessing the efficiency by performing the novel method technique.

4.2 Experimental results for classification technique

In this section, the test outcomes the classification procedure on the brain CT images are furnished. In CT images, the tumour and the non-tumour segments are classified with the help of SVM classifier. The novel approach is well-equipped to classify the tumour and non-tumour segments in an effectual manner. Figure 3 exhibits the CT test images with the authentication procedures guaranteeing superb precision.

Figure 3 Classification images

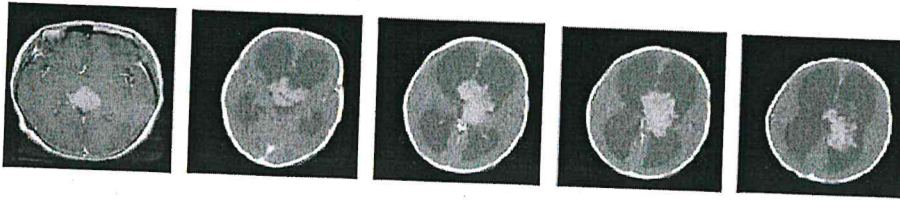
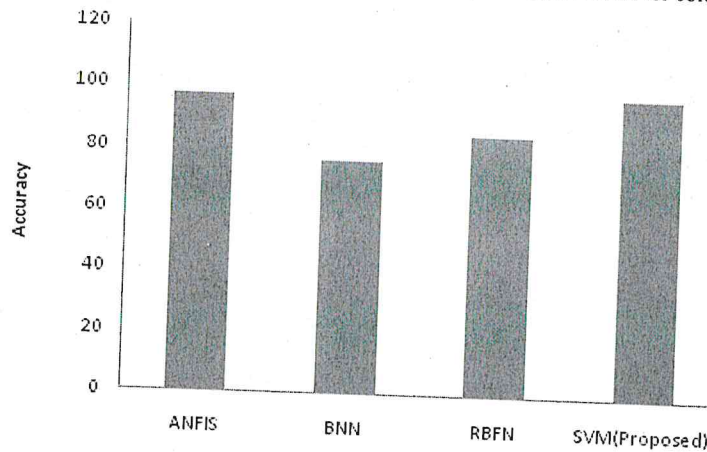


Figure 4 Classification of accuracy for different methods (see online version for colours)



In Figure 4, the classification of accuracy for different methods is shown above. The accuracy value is varying 0 to 120 comparing of ANFIS, BNN, RBFN and SVM proposed method. The ANFIS is 98%, BNN value is 78%, RBFN value is 88% and proposed SVM value is 99%. Generally the SVM value is higher than other techniques.

4.3 Segmentation performance

In the segmentation procedure, the tumour part is fragmented by novel approach viz. FCM with the centroid optimisation. This is done by employing the SSO. In Table 1, the original CT images housing the tumour and the fragmented tumour part of CT images are exhibited effectively. In the testing stage, the test dataset is furnished to the innovative method. This serves the purpose of locating the tumours in brain images and achieves the outcomes. The segmentation task includes the original image, the classified tumour image and fragmented image along with the performance measures like the sensitivity, specificity, accuracy, RI, global contingency error (GCE) and the VI. These evaluations are expressed in terms of various parameters such as TP, TN, FP and the FN.

- TP: tumour part correctly marked as tumour
- TN: normal area correctly unmarked as tumour
- FP: normal area wrongly marked as tumour
- FN: tumour area wrongly unmarked as tumour.

Table 2 shows the segmentation results of proposed and existing methods with sensitivity. In image 1, the proposed sensitivity value is 93.85% and existing value is 93.65%, whereas in image 2 the proposed sensitivity value is 95.08% and existing value is 93.10%. Image 3 shows the proposed sensitivity value as 90.36% and existing value as 88.30%, the image 4 proposed sensitivity values is 97.87% and existing value is 97.22%. Finally, image 5 proposed sensitivity value is 95.65% and existing value is 94.60%. The overall process shows the sensitivity of proposed FCM – (SSO + GA) as higher than other performance and existing FCM – (GWO) method.

Table 2 Segmentation results of proposed and existing methods with sensitivity











Sl. no	Original image	Segmented image	Sensitivity	
			FCM – (SSO + GA) (proposed)	FCM (GWO) (existing)
1			93.85%	93.65%
2			95.08%	93.10%
3			90.36%	88.30%
4			97.87%	97.22%
5			95.65%	94.60%

Table 3 shows the performance measures of FCM – (GWO) and FCM – (SSO + GA). The accuracy, specificity, RI, global consistency error (GCE) and VI values is predicted.

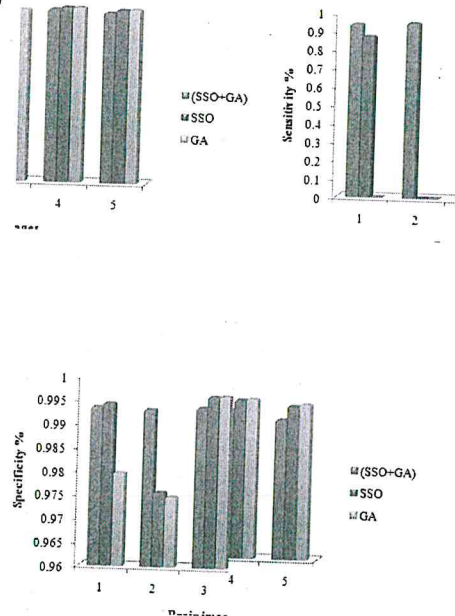
Table 3 Statistical performance measures of FCM – (GWO) and FCM – (SSO + GA)

Image no.	Accuracy		Specificity		RI		GCE		VI	
	FCM – (SSO + GA)	FCM – (GWO)	FCM – (SSO + GA)	FCM – (GWO)	FCM – (SSO + GA)	FCM – (GWO)	FCM – (SSO + GA)	FCM – (GWO)	FCM – (SSO + GA)	FCM – (GWO)
1	0.9928	0.992	0.9936	0.993	0.9856	0.985	0.0138	0.013	0.1686	0.170
2	0.9925	0.994	0.9933	0.9955	0.985	0.988	0.0143	0.010	0.1923	0.193
3	0.9907	0.991	0.9939	0.9953	0.9807	0.98	0.0147	0.018	0.3305	0.339
4	0.9913	0.992	0.9917	0.9932	0.9815	0.983	0.0169	0.01	0.326	0.3245
5	0.9893	0.991	0.9899	0.992	0.9785	0.981	0.0208	0.017	0.2341	0.2241

4.4 Comparison performance of three optimisation techniques

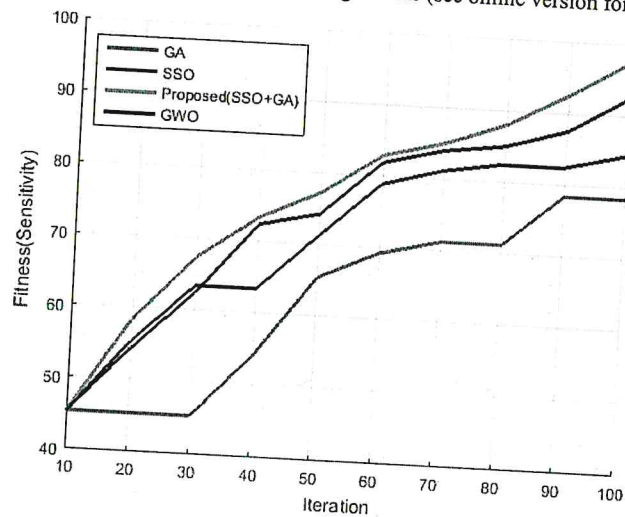
Figure 5 demonstrates the comparative performance of three optimisation techniques is shown. In this graph, the accuracy, sensitivity and specificity performance for different techniques namely (SSO with GA), SSO and GA algorithm is applied where the sensitivity value of SSO with GA is higher than SSO and GA algorithms.

Figure 5 Comparison performance of three optimisation techniques (see online version for colours)



4.5 Convergence graph for three algorithms

Figure 6 shows the convergence graph for different optimisation techniques. In this, the fitness of sensitivity varies from 40 to 100 and the iteration varies 10 to 100. The GA starts from fitness 45 and is constant up to 30th iteration. It slightly increases fitness 71 of iteration 70th and constant to 80th iteration with an increase in to fitness 89 of 90th iteration then constant to 100th iteration. In SSO algorithm there is fitness 45 of 10th iteration and it is improved to fitness 84 of 100th iteration. In GWO, the sensitivity fitness 45 is start and is increased to fitness 92 of 100th iteration. The proposed (SSO + GA) also starts from fitness 45 and is slightly raised up to fitness 99 of 100th iteration. In this graph, the fitness of sensitivity for proposed (SSO + GA) is higher to other comparative algorithms.

Figure 6 Convergence graph for optimisation algorithms (see online version for colours)

5 Conclusions

The two major challenges in the medical image segmentation are tumour image segmentation and classification. In this section, employing SVM helps to develop the model to detect the tumour part in brain images with an eye on classifying the tumour and non-tumour images. This is followed by the task of optimisation for FCM in relation to the segmentation procedure. In the above document, the SSO with GA is effectively employed to fragment the tumour part in the segmentation section is to fine-tune the segmentation function. The tumour recognition outcome is authenticated by means of the estimation tools such as sensitivity, specificity and the accuracy. In comparison with the existing classification method (ANFIS) the proposed (SVM) performs better in this paper. The sensitivity of SSO with GA optimisation technique value is 99% which was higher than specificity and accuracy values. In future various classification and optimisation techniques are to be used for enhanced performance. Regardless of the developing essentialness of advances in the medicinal services supply chains, minimal orderly understanding exists on the joining of advances, the determination or execution ramifications of innovation joining. Subsequently, in future, this prescribed strategy can be effectively connected to the next imaging modalities too for mind tumour location. This promising technique can be made to work upon the general execution of alternate classifiers utilised at the place of SVM in enhancing the precision. The exactness level has obviously revealed that the proposed calculation is exceptionally proficient in identifying the tumour-influenced parts in the cerebrum CT pictures.

With these lines, accepted firm that the proposed technique made alive will set up an appreciated point of interest other than acquiring yet another turning point in the field of biomedical building and in the historical backdrop of humanism and humankind also!

To accomplish better expectation rate, slope with HPF (high pass sifting) can be utilised as it noticeably give us edges with higher exactness.

References

- Al-Azzawi, N.A. and Sabir, M.K. (2015) 'An superior achievement of brain tumor detection using segmentation based on f-transform', in *2015 World Symposium on Proceedings of Computer Networks and Information Security (WSCNIS)*, IEEE, pp.1–5.
- Aslama, A., Khanb, E. and Beg, S. (2015) 'improved edge detection algorithm for brain tumor segmentation', in *Proceedings of Procedia Computer Science*, Vol. 58, pp.430–437.
- Aswathy, S.U., Dhas, G.G.D. and Kumar, S.S. (2014) 'A survey on detection of brain tumor from MRI brain images', in *2014 International Conference on IEEE Control, Instrumentation, Communication and Computational Technologies (ICCICCT)*, pp.871–877.
- Capelle, A.S., Colot, O. and Fernandez-Maloigne, C. (2004) 'Evidential segmentation scheme of multi-echo MR images for the detection of brain tumors using neighborhood information', *Information Fusion*, Vol. 5, No. 3, pp.203–216.
- Chandra, R. and Ramchand, K. (2016) 'Tumor detection in brain using genetic algorithm', in *Proceedings of Procedia Computer Science*, Vol. 79, pp.449–457.
- Charutha, S. and Jayashree, M.J. (2014) 'An efficient brain tumor detection by integrating modified texture based region growing and cellular automata edge detection', in *Proceedings of Control, Instrumentation, Communication and Computational Technologies (ICCICCT)*, pp.1193–1199.
- Chawla, M. and Duhan, M. (2014) 'Applications of recent metaheuristics optimisation algorithms in biomedical engineering: a review', *International Journal of Biomedical Engineering and Technology*, Vol. 16, No. 3, pp.268–278.
- Deepa, T., Sathiyabhama, B., Akilandeswari, J. and Gopalan, N.P. (2014) 'Action fuzzy rule based classifier for analysis of dermatology databases', *International Journal of Biomedical Engineering and Technology*, Vol. 15, No. 4, pp.360–379.
- Dvorak, P., Kropatsch, W. and Bartusek, K. (2013) 'automatic detection of brain tumors in MR images', in *Proceedings of Telecommunications and Si 2013*, (TSP) IEEE, pp.577–580.
- Gandhi, T., Swami, P., Santhosh, J. and Anand, S. (2011) 'Dynamical neural activation in human brain during face recognition', *International Journal of Biomedical Engineering and Technology*, Vol. 7, No. 2, pp.135–147.
- Ghanavati, S., Li, J., Liu, T., Babyn, P.S., Doda, W. and Lampropoulos, G. (2012) 'Automatic brain tumor detection in magnetic resonance images', in *2012 9th IEEE International Symposium on Biomedical Imaging (ISBI)*, IEEE, pp.574–577.
- Halder, A., Giri, C. and Halder, A. (2014) 'Brain tumor detection using segmentation based object labeling algorithm', in *Proceedings of Electronics, Communication and Instrumentation (ICECI)*, pp.1–4.
- Hamamci, A., Kucuk, N., Karaman, K., Engin, K. and Unal, G. (2012) 'Tumor-cut: segmentation of brain tumors on contrast enhanced MR images for radiosurgery applications', *Journal of IEEE Transactions On Medical Imaging*, Vol. 31, No. 3, pp.790–804.
- Iftekharruddin, K.M., Zheng, J., Islam, M.A. and Ogg, R.J. (2009) 'Fractal-based brain tumor detection in multimodal MRI', *Applied Mathematics and Computation*, Vol. 207, No. 1, pp.23–41.
- Kanas, V., Zacharaki, E., Davatzikos, C., Sgarbas, K. and Megalooikonomou, V. (2015) 'A low cost approach for brain tumor segmentation based on intensity modeling and 3D random walker', *Journal of Biomedical Signal Processing and Control*, Vol. 22, pp.19–30.
- Kavitha, A.R. and Chellamuthu, C. (2013) 'Detection of brain tumour from MRI image using modified region growing and neural network', *Journal of Imaging Science*, Vol. 61, No. 7, pp.556–567.
- Lemieux, L., Hagemann, G., Krakow, K. and Woermann, F. (1999) 'Fast, accurate, and reproducible automatic segmentation of the brain in T1-weighted volume MRI data', *Journal of Magnetic Resonance in Medicine*, Vol. 42, No. 1, pp.127–135.

- Lim, L.G., Naguib, R. and Dadios, E. (2010) 'Image classification of microscopic colonic images using textural properties and KSOM', *International Journal of Biomedical Engineering and Technology*, Vol. 3, No. 3, pp.308–318.
- Majo, C., Julia-Sape, M., Alonso, J., Serrallonga, M., Aguilera, C., Acebes, J., Aru, C. and Gili, J. (2004) 'Brain tumor classification by proton MR spectroscopy: comparison of diagnostic accuracy at short and long TE', *Journal of American Journal of Neuroradiology*, Vol. 25, No. 10, pp.1696–1704.
- Murray, J.D. (2012) 'Glioblastoma brain tumours: estimating the time from brain tumour initiation and resolution of a patient survival anomaly after similar treatment protocols', *Journal of Biological Dynamics*, Vol. 6, No. 2, pp.118–127.
- Murugesan, M. and Sukanesh, R. (2009) 'Automated detection of brain tumor in EEG signals using artificial neural networks', in *Proceedings of Conference on Advances in Computing, Control, and Telecommunication Technologies*, pp.284–288.
- Padma, A. and Sukanesh, R. (2011) 'Automatic classification and segmentation of brain tumor in CT images using optimal dominant gray level run length texture features', *International Journal of Advanced Computer Science and Applications*, Vol. 2, No. 10, pp.23–29.
- Poonguzhali, S. and Ravindran, G. (2007) 'Evaluation of feature extraction methods for classification of liver abnormalities in ultrasound images', *International Journal of Biomedical Engineering and Technology*, Vol. 1, No. 2, pp.134–143.
- Porz, N., Bauer, S., Pica, A., Schucht, P., Beck, J., Verma, R.K., Slotboom, J., Reyes, M. and Wiest, R. (2014) 'Multi-modal glioblastoma segmentation: man versus machine', *PloS One*, Vol. 9, No. 5.
- Preetha, R. and Suresh, G.R. (2014) 'Performance analysis of fuzzy C means algorithm in automated detection of brain tumor', in *Proceedings of Computing and Communication Technologies (WCCCT)*, pp.30–33.
- Rajalakshmi, N. and Prabha, V.L. (2015) 'Segregation of MRI brain image using hybrid evolutionary clustering algorithm', *International Journal of Biomedical Engineering and Technology*, Vol. 18, No. 1, pp.30–51.
- Rajasekaran, M.P. and Sri Meena, R. (2012) 'Application of adaptive neuro-fuzzy inference systems for MR image classification and tumor detection', *International Journal of Biomedical Engineering and Technology*, Vol. 9, No. 2, pp.133–146.
- Renjith, A., Manjula, P. and Mohan Kumar, P. (2015) 'Brain tumor classification and abnormality detection using neuro-fuzzy technique and Otsu thresholding', *Journal of Medical Engineering & Technology*, Vol. 39, No. 8, pp.498–507.
- Senthilkumar, V. and Ezhilarasi, M. (2016) 'An efficient multi-RVM classification-based ultrasound lung image retrieval approach', *International Journal of Biomedical Engineering and Technology*, Vol. 22, No. 3, pp.189–215.
- Shanthakumar, P. and Ganeshkumar, P. (2015) 'Performance analysis of classifier for brain tumor detection and diagnosis', *Journal of Computers & Electrical Engineering*, Vol. 45, pp.302–311.
- Singla, R.K., Khosla, A. and Jha, R. (2014) 'Influence of stimuli colour on feature classification for BCI applications', *International Journal of Biomedical Engineering and Technology*, Vol. 15, No. 1, pp.82–93.
- Suganami, A., Iwadated, Y., Shibataa, S., Yamashitaf, M., Tanakaf, T., Shinozakid, N., Aokie, I., Saekid, N., Shirasawab, H., Okamoto, Y. and Tamura, Y. (2015) 'Liposomally formulated phospholipid-conjugated indocyanine green for intra-operative brain tumor detection and resection', *Journal of Pharmaceutics*, Vol. 496, pp.401–406.
- Yacin, S.M. and Vennila, M. (2015) 'Analysis of fetal electrocardiogram extraction methods and enhancement using Hilbert-Huang transform', *International Journal of Biomedical Engineering and Technology*, Vol. 18, No. 1, pp.14–29.
- Zeljko, V., Druzgalski, C., Zhang, Y., Zhu, Z., Xu, Z., Zhang, D. and Mayorga, P. (2014) 'Automatic brain tumor detection and segmentation in MR images', in *2014 Pan American Health Care Exchanges (PAHCE)*, IEEE, pp.1–1.